Dalton Transactions

COMMUNICATION

View Article Online
View Journal | View Issue

Cite this: *Dalton Trans.*, 2016, **45**, 16556

Received 5th May 2016,
Accepted 20th May 2016

DOI: 10.1039/c6dt01763k

www.rsc.org/dalton

Magnetic frustration in a hexaazatrinaphthylene-bridged trimetallic dysprosium single-molecule magnet†

Richard Grindell,[a] Veacheslav Vieru,[b] Thomas Pugh,[a] Liviu F. Chibotaru*[b] and Richard A. Layfield*[a]

The synthesis, structure and magnetic properties of the HAN-bridged tri-dysprosium complex [{(thd)$_3$Dy}$_3$HAN] (1) are described. The complex is an SMM that shows two relaxation processes owing to the presence of two geometrically distinct Dy^{3+} sites in 1. *Ab initio* calculations reveal that the magnetic ground state of 1 is characterized by magnetic frustration.

Single-molecule magnets (SMMs) are molecular species that show magnetic bistability which, for a true SMM, results in magnetic hysteresis being observed up to a characteristic blocking temperature, T_B.[1] The properties of SMMs are typically rationalized in terms of correlations between the molecular and electronic structures of individual molecules,[2] making such species distinct from classical atom-based inorganic magnets, in which long-range ordering is important.

Studies of SMMs have generated a significant amount of fundamental insight into the properties of highly anisotropic molecular magnets. A strong indication that the field has reached a stage of maturity is that new research areas have begun to emerge from within single-molecule magnetism. One of the most exciting recent developments has been the incorporation of some SMMs into spintronic devices.[3] Most prominent amongst the applications of SMMs in molecular spintronics are sandwich-like terbium(III) complexes of phthalocyanine ligands, which have been used in, for example, molecular spin valves[4] and devices that allow the coherent manipulation of individual nuclear spins using an electric field.[5]

An intriguing subset of SMMs that may offer an alternative approach to applications of molecular magnets in nanoscale devices are the so-called single-molecule toroics (SMTs).[6] SMTs are polymetallic cage compounds possessing an overall toroidal magnetic moment, which arises from a vortex-like, non-collinear arrangement of the individual moments. To date, SMT properties have been identified in several dysprosium-containing cage compounds with nuclearities of up to Dy_6,[7,8] but SMT behaviour is most prominent in trimetallic compounds.[9] Indeed, the first species found to display a toroidal magnetic moment was the complex cation $[Dy_3(\mu_3\text{-}OH)_2(ovn)_3Cl_2(H_2O)_4]^{2+}$ (ovn = *ortho*-vanillin): notably, in this SMT and in all subsequent examples, the toroidal magnetism was identified through the use of *ab initio* calculations.[10]

Although toroidal magnetism has been observed in several triangular Dy_3 complexes, such arrangements of spin centres are no guarantee that the phenomenon will occur. Targeting SMT behaviour in a rational way is challenging but not impossible, and to achieve this aim further insight into the relationship between the molecular and electronic structure of trimetallic dysprosium complexes is required. We have developed an interest in the tritopic hexazaatrinaphthylene (HAN, Scheme 1) family of ligands,[11] the three-fold symmetry of which could provide a platform on which to construct toroidal magnetism and to search for phenomena such as frustrated magnetism. Thus, we targeted a tri-dysprosium complex of HAN, which was achieved with the synthesis of [{(thd)$_3$Dy}$_3$HAN] (**1**), where thd is 2,2,6,6-tetramethylheptanedionate (Scheme 1).

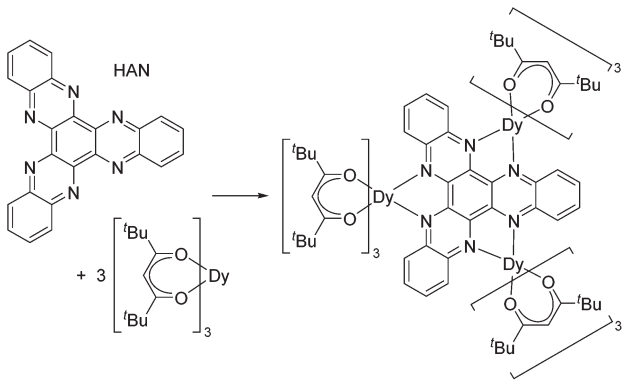

Scheme 1 Synthesis of [{(thd)$_3$Dy}$_3$HAN] (**1**).

[a]*School of Chemistry, The University of Manchester, Oxford Road, Manchester, M13 9PL, UK. E-mail: Richard.Layfield@manchester.ac.uk*
[b]*Theory of Nanomaterials Group, Katholieke Universiteit Leuven, Celestijenlaan 200F, 3001 Heverlee, Belgium. E-mail: Liviu.Chibotaru@chem.kuleuven.be*

†Electronic supplementary information (ESI) available: Synthetic details, spectroscopic characterization, X-ray crystallography details and crystallographic information file, computational details. CCDC 1478313. For ESI and crystallographic data in CIF or other electronic format see DOI: 10.1039/c6dt01763k

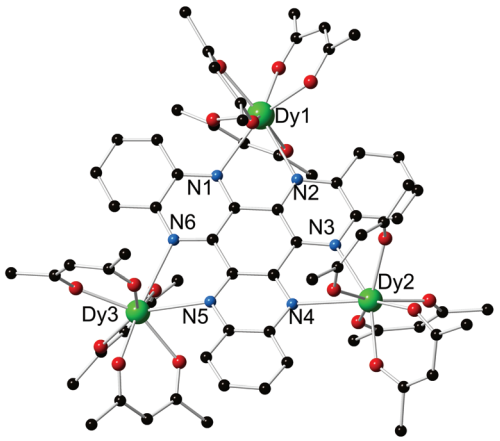

Fig. 1 Molecular structure of **1**. For clarity, the methyl groups on the $[thd]^-$ ligands and the hydrogen atoms are not shown.

Compound **1**·3(toluene) was isolated as dark red crystals in a yield of 86%, and the molecular structure was determined by X-ray crystallography (Fig. 1, Table S1†). The three dysprosium centres in **1** reside in DyO_6N_2 environments by virtue of three bidentate $[thd]^-$ ligands and two nitrogen donors of the HAN ligand. For Dy(1), the Dy–O distances lie in the range 2.256(5)–2.342(5) Å, and for Dy(2) and Dy(3) the analogous distances are 2.251(6)–2.315(6) Å and 2.259(5)–2.318(5) Å (Table S2†). The Dy–N distances in **1** are 2.646(6)–2.760(6) Å. Although the dysprosium centres are not symmetry related, Dy(1) and Dy(2) occupy similar positions with respect to the plane of the six HAN nitrogen donor atoms. In contrast, Dy(3) is displaced out of the N_6 plane by 1.044 Å. The Dy(1)···Dy(2), Dy(1)···Dy(3) and Dy(2)···Dy(3) separations are 8.100(10) Å, 8.147(10) Å and 8.118(9) Å, respectively.

The metric parameters for the dysprosium centres were analysed using the SHAPE software,[12] which revealed that the DyO_6N_2 environments can be described as distorted dodecahedra. Thus, the CShM values for Dy(1), Dy(2) and Dy(3) with respect to D_{2d} symmetry are 0.840, 1.624 and 1.797, implying that the latter two metal centres occupy very similar geometries, both of which are more distorted from ideal dodecahedral than that of Dy(1).

Although transition metal complexes of the HAN family of ligands are well known,[13] studies of their magnetic properties are uncommon. Recent examples include two-step spin-crossover in the chiral coordination polymer $[Fe(HAT)(NCS)_2]_\infty$ (HAT = hexaazatriphenylene)[14] and the cobalt(II) species $[K(18\text{-}c\text{-}6)][(HAN)\{Co(N'')_2\}_3]$, which contains the radical anionic $[HAN]^{\bullet-}$ ligand.[11a] Compound **1** is the first tri-lanthanide complex of this type of tritopic ligand.

The molar magnetic susceptibility (χ_M) of **1**·3(toluene) was measured in a static field of H_{dc} = 1 kOe in the temperature range 2–300 K (Fig. S4†). At 300 K, $\chi_M T$ is 41.57 cm^3 K mol^{-1}, which is consistent with the value of 42.51 cm^3 K mol^{-1} predicted for three non-interacting Dy^{3+} ions with $^6H_{15/2}$ ground terms and g = 4/3. As the temperature is lowered, $\chi_M T$ slowly decreases to reach 37.65 cm^3 K mol^{-1} at 50 K, and at lower temperatures, $\chi_M T$ decreases more rapidly and reaches 16.42 cm^3 K mol^{-1} at 2 K. The temperature dependence of $\chi_M T$ can, in principle, be assigned to a combination of antiferromagnetic exchange between the dysprosium centres and the depopulation of the excited Kramers doublets within the spin–orbit coupled ground term.

The field dependence of the magnetization (M) was measured at various intervals in the range 0–70 kOe and at temperatures of 1.8, 3, 5, and 8 K (Fig. S5†). For the measurement at 1.8 K, the magnetization increases sharply as the field increases to 10 kOe before levelling off and reaching a value of M = 15.54μ_B at 70 kOe, which agrees well with the expected value of 15.75μ_B for three Dy^{3+} ions. Using a field sweep rate of 1.9 mT s^{-1}, the magnetic hysteresis of **1** was also investigated at 1.8 and 2.2 K, which revealed S-shaped loops that close around zero field (Fig. S12†).

Next, we examined the magnetic properties **1**·3(toluene) using an alternating current (a.c.) magnetic field of H_{ac} = 1.55 Oe, initially with zero applied d.c. field. The in-phase (χ') and the out-of-phase (χ'') susceptibilities were measured as functions of the frequency of the oscillating field (ν) at 1 K intervals in the range 2–19 K (Fig. S6†). The plot of $\chi''(\nu)$ (Fig. 2) at 2 K is double-humped, which indicates SMM behaviour with two regimes of thermal relaxation. The Argand plots of χ'' *vs.* χ' (Fig. S8†) confirm the occurrence of two relaxation processes, and the fits of these data with α parameters in the range 0.09–0.59 imply a wide range of relaxation times. As the temperature is raised the maximum of the higher frequency process shifts to frequencies greater than can be achieved with our SQUID magnetometer, whereas the maximum in the lower-frequency process is discernible up to 10 K.

Conducting the $\chi''(\nu)$ measurement in an optimized d.c. field of 1 kOe allows both sets of maxima to be observed across a wider temperature range (Fig. 2 and S7†). For each relaxation process, the position of the maximum in χ'' shifts markedly to higher frequencies as the temperature is increased, indicating that two independent thermal relaxation processes occur simultaneously. Qualitatively, this observation can be rationalised in terms of the two types of dodecahedral Dy^{3+} coordination environments in **1**.

Further insight into the a.c. susceptibility of **1** was obtained from the relationship between the relaxation time, τ, and temperature, which yields the effective energy barrier to reversal of the magnetization, U_{eff}, *via* $\tau = \tau_0 \exp(-U_{eff}/k_B T)$. The plot of ln τ *versus* T^{-1} for the zero-field data (Fig. S11†) presents an irregular series of data points, which is a consequence of the overlapping $\chi''(\nu)$ curves. Although an anisotropy barrier of 22 cm^{-1} can be extracted from these data ($\tau_0 = 8.2 \times 10^{-6}$ s), the physical significance of this number is limited. In contrast, the in-field data allow two well-defined thermal relaxation processes to be characterised (Fig. 3), with modest anisotropy barriers of U_{eff} = 42 cm^{-1} and 52 cm^{-1} ($\tau_0 = 3.8 \times 10^{-6}$ s and 5.6×10^{-6} s), respectively. The occurrence of two relaxation processes in SMMs containing more than one type of dysprosium environment has been described previously in various polynuclear systems.[15]

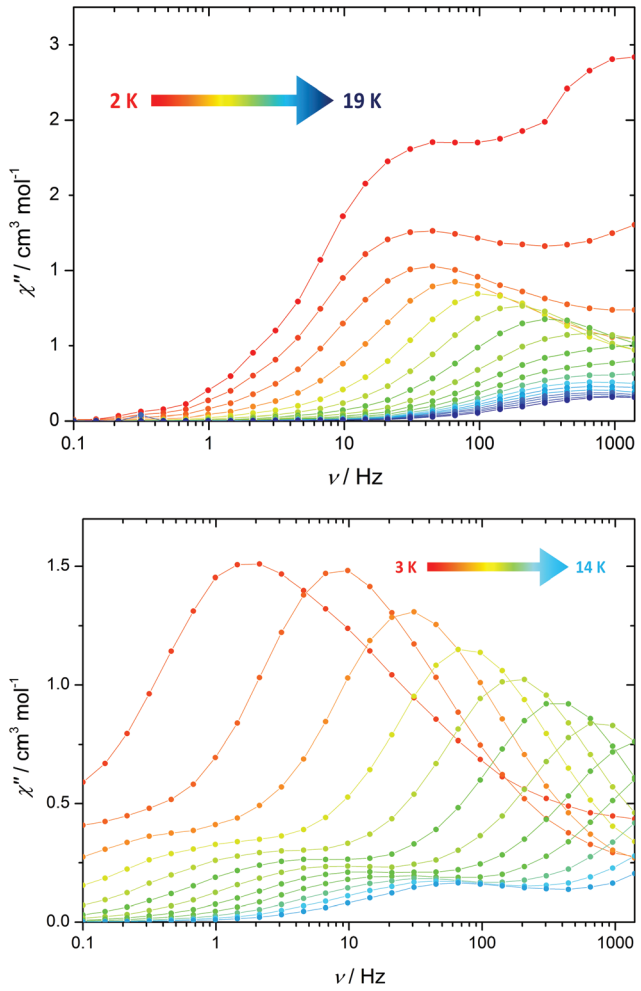

Fig. 2 Frequency dependence of χ'' for **1** in zero d.c. field (upper) and H_{dc} = 1 kOe (lower).

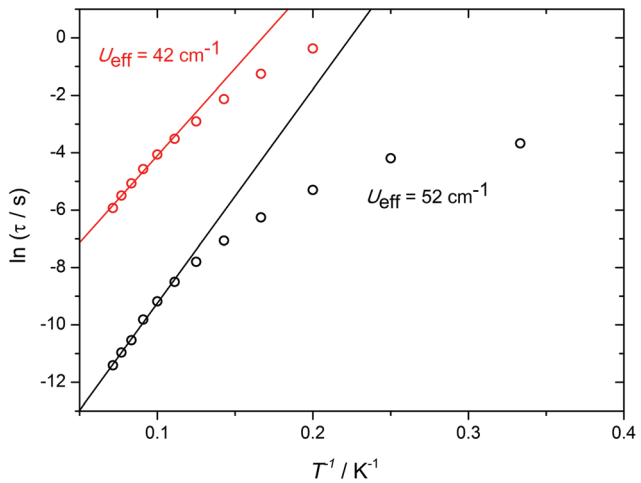

Fig. 3 Plots of ln τ *vs.* 1/T for **1** in an applied field of 1 kOe. The solid lines represent fits to the high-temperature data.

In order to develop a detailed picture of the electronic structure of **1**, *ab initio* calculations of the CASSCF/RASSI type were performed using the MOLCAS software.[16] Three separate [{(thd)$_3$Dy}HAN] fragments were considered in the calculations (Fig. S13†). The energies of the eight lowest-lying Kramers doublets (KDs) for each Dy^{3+} centre are shown in Table 1, which reveals that the subtle differences in the coordination environments have a clear impact on the energies of the crystal field levels. The different energies for the KDs of the three Dy^{3+} centres reflect the fact that they are not related by crystallographic symmetry. The calculated energy gaps from ground to first-excited KD are somewhat larger than the experimentally extracted values, which might indicate that the relaxation is not of a purely activated type.

The calculated *g*-tensors for the ground KD of each Dy^{3+} reveal strong magnetic anisotropy approach the Ising limit for dysprosium, *i.e.* g_z = 20 and $g_{x,y}$ = 0 (Tables 1 and S5†). The calculations also provide a very convenient method for visualizing the orientation of the magnetic axis for the various KDs. Thus, it can be seen in Fig. 4 that the magnetic axes in the ground KDs are oriented at angles of 82°, 68° and 71° with respect to

Table 1 Energies (cm^{-1}) of the lowest-lying Kramers doublets for the Dy^{3+} centres in **1** and *g*-tensors for the ground doublets

KD	Dy(1)	Dy(2)	Dy(3)
1	0	0	0
2	121	152	64
3	238	252	177
4	314	336	279
5	379	421	369
6	446	505	470
7	549	627	542
8	710	794	621
g_x	0.016	0.001	0.009
g_y	0.030	0.005	0.018
g_z	19.290	19.950	19.120

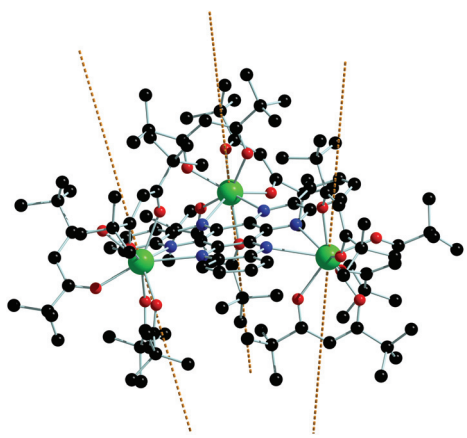

Fig. 4 Orientation of the main magnetic axes (dashed lines) in the ground Kramers doublets of **1**. Dy = green, N = blue, O = red, C = grey (hydrogen atoms omitted for clarity).

Table 2 Ising parameters (cm^{-1}) for **1**

	J_{ex}	J_{dip}
Dy(1)–Dy(2)	−2.3	−0.29
Dy(1)–Dy(3)	−2.5	−0.29
Dy(2)–Dy(3)	−2.5	−0.28

the N_6 plane of the HAN ligand, suggesting that the $[thd]^-$ ligands dominate the ligand field, whereas the N-donors of the HAN ligand play a relatively minor role. The orientations of the main magnetic axes on the Dy^{3+} centres in **1** are consistent with that calculated for the related monometallic species $[(thd)_3Dy(1,10\text{-phenanthroline})]$.[17] Consequently, such an arrangement of magnetic moments does not meet one of the indispensible conditions for an overall toroidal moment, *i.e.* that the individual anisotropy axes are co-planar.

The calculations also allow the total magnetic interactions in **1** to be accounted for, which was achieved using the following Hamiltonian:

$$\hat{H} = -[(J_{12}^{dip} + J^{exch})\hat{\tilde{s}}_{1,z1}\hat{\tilde{s}}_{2,z2} + (J_{13}^{dip} + J^{exch})\hat{\tilde{s}}_{1,z1}\hat{\tilde{s}}_{3,z3} + (J_{23}^{dip} + J^{exch})\hat{\tilde{s}}_{2,z2}\hat{\tilde{s}}_{3,z3}]$$

The Ising exchange parameters (J_{exch}) were calculated from Lines parameters by taking into account the angle between the main anisotropy axes of the interacting Dy^{3+} sites (see ESI† for details). The Lines parameters were determined by fitting the experimental susceptibility data (Fig. S14 and S15†). The dipolar parameters were calculated straightforwardly (Table 2).

Thus, the dipolar and exchange components, and hence the overall interactions between the pairs of Dy^{3+} ions, are antiferromagnetic in nature. Furthermore, the energies of the six lowest energy exchange states (*i.e.* three doublets) in **1** (Table S7†) are all approximately equal to zero, suggesting that the magnetic ground state is frustrated. This property is reminiscent of the frustration observed in the endohedral fullerene $Dy_3N@C_{80}$,[18] and in the trimetallic dysprosium SMMs $[Cp'_2Dy(\mu\text{-}X)]_3$, where X contains a soft donor atom, *e.g.* phosphorus, arsenic, sulphur or selenium ($Cp' = C_5H_4Me$).[19]

Conclusions

In conclusion, $[\{(thd)_3Dy\}_3HAN]$ (**1**), the first tri-lanthanide complex of the HAN family of ligands, has been synthesized through a rationally designed synthetic method. Dynamic magnetic susceptibility measurements in zero applied field reveal SMM behaviour and the occurrence of two overlapping relaxation processes, which can be resolved in an applied field of 1 kOe. Modest anisotropy barriers of 42 cm^{-1} and 52 cm^{-1} were determined, with the two processes being consistent with the presence of two different types of distorted dodecahedral DyO_6N_2 environments in **1**.

Ab initio calculations reveal that the main magnetic axes on the Dy^{3+} centres are oriented approximately perpendicular to the HAN ligand, which precludes SMT properties. However, the antiferromagnetic exchange between pairs of dysprosium ions in **1** allow this complex to be regarded as a frustrated spin system. Studies aimed at enhancing the exchange interactions between the metal centres in **1** through the use of radical derivatives of HAN are underway.

Acknowledgements

R. A. L., L. F. C. and T. P. thank the ERC for the Consolidator Grant 'RadMag' (646740). R. A. L. thanks UK EPSRC for Core Capability Grant EP/K039547/1. L. F. C. and V. V. acknowledge the Belgium Science Foundation (FWO) and the Concerted Action Scheme (GOA) of KU Leuven. The authors also thank Dr Fu-Sheng Guo (Manchester) for useful discussions.

Notes and references

1 (*a*) P. Zhang, L. Zhang and J. Tang, *Dalton Trans.*, 2014, **44**, 3923; (*b*) D. N. Woodruff, R. E. P. Winpenny and R. A. Layfield, *Chem. Rev.*, 2013, **113**, 5110; (*c*) K. S. Pedersen, J. Bendix and R. Clérac, *Chem. Commun.*, 2014, **50**, 4396; (*d*) J. M. Frost, K. L. M. Harriman and M. Murugesu, *Chem. Sci.*, 2016, **7**, 2470; (*e*) R. A. Layfield, *Organometallics*, 2014, **33**, 1084.
2 (*a*) J. Liu, Y.-C. Chen, J.-L. Liu, V. Vieru, L. Ungur, J.-H. Jia, L. F. Chibotaru, Y. Lan, W. Wernsdorfer, S. Gao, X.-M. Chen and M.-L. Tong, *J. Am. Chem. Soc.*, 2016, **138**, 5441; (*b*) S. K. Gupta, T. R. Kumar, G. Rajaraman and R. Murugavel, *Chem. Sci.*, DOI: 10.1039/c6sc00279j.
3 L. Bogani, *Struct. Bonding*, 2015, **164**, 331.
4 M. Urdampilleta, S. Klayatskaya, M. Ruben and W. Wernsdorfer, *ACS Nano*, 2015, **9**, 4458.
5 S. Thiele, F. Balestro, R. Ballou, S. Klyatskaya, M. Ruben and W. Wernsdorfer, *Science*, 2014, **344**, 1135.
6 L. Ungur, S.-Y. Lin, J. Tang and L. F. Chibotaru, *Chem. Soc. Rev.*, 2014, **43**, 6894.
7 I. J. Hewitt, J. Tang, N. T. Madhu, C. E. Anson, Y. Lan, J. Luzon, M. Etienne, R. Sessoli and A. K. Powell, *Angew. Chem., Int. Ed.*, 2010, **49**, 6352.
8 L. Ungur, S. K. Langley, T. N. Hooper, B. Moubaraki, E. K. Brechin, K. S. Murray and L. F. Chibotaru, *J. Am. Chem. Soc.*, 2012, **134**, 18554.
9 J. Tang, I. Hewitt, N. T. Madhu, G. Chastanet, W. Wernsdorfer, C. E. Anson, C. Benelli, R. Sessoli and A. K. Powell, *Angew. Chem., Int. Ed.*, 2006, **45**, 1729.
10 L. F. Chibotaru, L. Ungur and A. Soncini, *Angew. Chem., Int. Ed.*, 2008, **47**, 4126.
11 (*a*) J. O. Moilanen, N. F. Chilton, B. M. Day, T. Pugh and R. A. Layfield, *Angew. Chem., Int. Ed.*, 2016, **55**, 5521; (*b*) J. O. Moilanen, B. M. Day, T. Pugh and R. A. Layfield, *Chem. Commun.*, 2015, **51**, 11478.
12 *SHAPE Continuous Measures Calculation, version 2.1*, Universitat de Barcelona, 2013.

13 S. Kitagawa and S. Masaoka, *Coord. Chem. Rev.*, 2003, **246**, 73.
14 T. Romero-Morcillo, F. J. Valverde-Muñoz, M. Carmen Muñoz, J. M. Herrera, E. Colacio and J. A. Real, *RSC Adv.*, 2015, **5**, 69782.
15 (*a*) Y.-N. Guo, G.-F. Xu, P. Gamez, L. Zhao, S.-Y. Lin, R. Deng, J. Tang and H.-J. Zhang, *J. Am. Chem. Soc.*, 2008, **132**, 8538; (*b*) A. Venugopal, F. Tuna, T. P. Spaniol, L. Ungur, L. F. Chibotaru, J. Okuda and R. A. Layfield, *Chem. Commun.*, 2013, **49**, 901.
16 (*a*) L. F. Chibotaru, L. Ungur, C. Aronica, H. Elmoll, G. Pilet and D. Luneau, *J. Am. Chem. Soc.*, 2008, **130**, 12445; (*b*) L. F. Chibotaru and L. Ungur, *J. Chem. Phys.*, 2012, **137**, 064112; (*c*) F. Aquilante, *et al.*, *J. Comput. Chem.*, 2016, **37**, 506.
17 (*a*) G.-J. Chen, C.-Y. Chao, J.-L. Tian, J. Tang, W. Gu, X. Liu, S.-P. Yan, D.-Z. Liao and P. Cheng, *Dalton Trans.*, 2011, **40**, 5579; (*b*) N. F. Chilton, D. Collison, E. J. L. McInnes, R. E. P. Winpenny and A. Soncini, *Nat. Commun.*, 2013, **4**, 2551; (*c*) Y. Ma, G.-F. Xu, X. Yang, L.-C. Li, J. Tang, S.-P. Yan, P. Cheng and D.-Z. Liao, *Chem. Commun.*, 2010, **46**, 8264.
18 V. Vieru, L. Ungur and L. F. Chibotaru, *J. Phys. Chem. Lett.*, 2013, **4**, 3565.
19 (*a*) T. Pugh, F. Tuna, L. Ungur, D. Collison, E. J. L. McInnes, L. F. Chibotaru and R. A. Layfield, *Nat. Commun.*, 2015, **6**, 7492; (*b*) T. Pugh, A. Kerridge and R. A. Layfield, *Angew. Chem., Int. Ed.*, 2015, **54**, 4255; (*c*) T. Pugh, V. Vieru, L. F. Chibotaru and R. A. Layfield, *Chem. Sci.*, 2016, **7**, 2128.